Langmuir

Article

pubs.acs.org/Langmuir

Design and Application of Anthracene Derivative with Aggregation-Induced Emission Charateristics for Visualization and Monitoring of Erythropoietin Unfolding

Binjie Sun,[†] Xiaojun Yang,[†] Lin Ma, Caixia Niu, Fangfang Wang, Na Na, Jiying Wen, and Jin Ouyang*

College of Chemistry, Beijing Normal University, Beijing 100875, China

Supporting Information

ABSTRACT: Erythropoietin (EPO) is an attractive protein-unfolding/folding model because of its high degree of unfolding and folding reversibility and intermediate size. Due to its function for regulating red blood cell production by stimulating late erythroid precursor cells, EPO presents obvious values to biological research. A nonemissive anthracene derivative, that is 9,10-bis[4-(3-sulfonatopropoxyl)-styryl]anthracene sodium salt (BSPSA), with aggregation-induced emission (AIE) charateristics shows a novel phenomenon of AIE when EPO is added. The AIE biosensor for EPO shows the limit of detection is 1×10^{-9} M. Utilizing the AIE feature of BSPSA, the unfolding process of EPO using guanidine hydrochloride is monitored, which indicates three steps for the folding structures of EPO to transform to random coil. Computational modeling suggests that the BSPSA luminogens prefer docking in the hydrophobic cavity in the EPO folding structures, and the assembly of BSPSA in this cavity makes the AIE available, making the monitoring of unfolding of EPO possible.

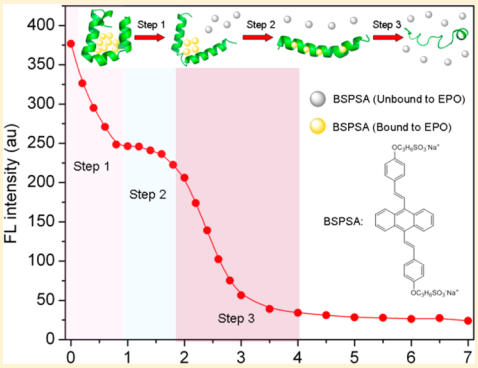

INTRODUCTION

Protein folding and unfolding are strategically important to secreted, membrane-bound, and cellular function.[1] It is well-known that studies for the conformation change of the protein are widely applied in functional studies of proteins, which significantly promote the understanding of the mystery of life, and developments in the field of clinical diagnostics.[2,3] The conformation studies also promote understanding the role of dynamics in the function of proteins,[4] involving motion of key residues[5] or large-scale domain movements,[6] which take place within the context of protein folding and unfolding. A transition between folded and unfolded structures is also required for function of some proteins.[7] Hence, understanding the mechanism and process of protein folding and unfolding is of fundamental importance for proteomic and pharmaceutical research.

Erythropoietin (EPO), produced primarily in the kidney of adults, is a glycoprotein hormone with multiple functions. It is usually used in treatment of cancer,[8] kidney dysfunction,[9] and nervous system injuries.[10] Unlike small molecular agents, protein pharmaceuticals must have the correct conformation to ensure bioactivity and efficacy. The conformation studies of EPO also provide a tool for understanding the intermolecular action between EPO and its receptor[11] or other bioactive molecules.[12] Meanwhile, because of its high degree of unfolding and folding reversibility and intermediate size, EPO conformation change is an attractive protein-unfolding/folding model for biological research.

Although the biological functions of proteins have a great relationship with its conformations and folding structures, to understand protein unfolding process is still a challenge. Different methods were developed in protein folding and unfolding studies like hydroxyl radical protein foot printing,[13] single molecule methods,[14] atomic force microscopy,[15] fluorescence,[16,17] high precision densimetric and ultrasonic measurements,[18] and force spectroscopy.[19] Since these methods lack appropriate probes, intermediate states which are suspected to be involved in the unfolding processes of many proteins are often not monitored.[20,21] Hence, the characterization of the intermediate states becomes difficult in proteins, especially in the multidomain proteins, such as EPO. Because each domain of EPO is capable of unfolding independently as other multidomain proteins,[22] the study of the intermediate states of EPO becomes more difficult. According to the literature we know, a two-state assumption model is usually adopted in kinetic and thermodynamic analysis of EPO unfolding studies.[23,24] In this model the unfolding process of EPO is believed to follow a single step, two states pathway, directly from a three-dimensional structure to one-dimensional structure. In such a model no intermediate state, which may be involved in protein unfolding process,[25] was considered. Advances, therefore, in the research of the intermediate states

Received: December 6, 2012
Revised: January 14, 2013
Published: January 16, 2013

Scheme 1. Synthetic Route of BSPSA[34]

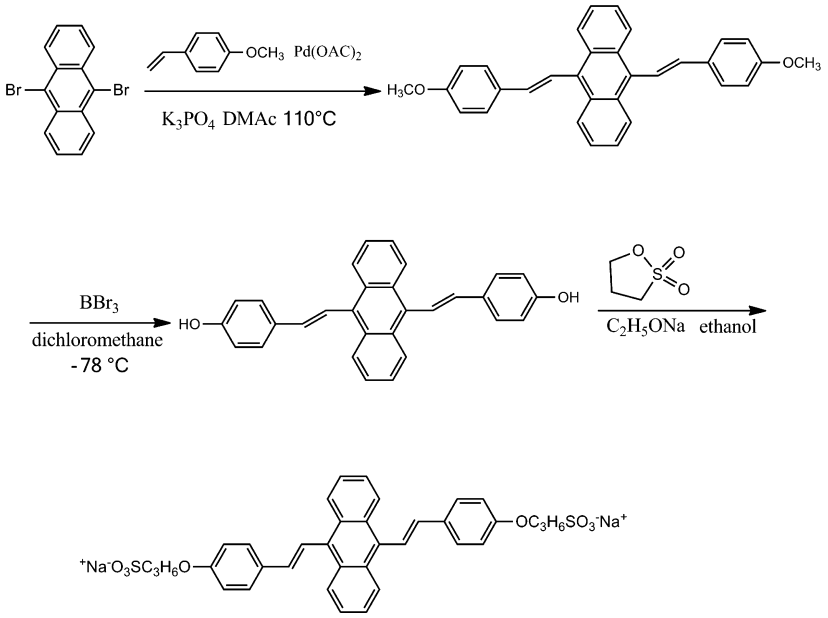

of EPO with an appropriate probe will be of crucial importance to study the function of EPO.

Recently, materials with aggregation-induced emission (AIE) properties are drawing the attention of more and more researchers.[26−29] Unlike the traditional fluorescence (FL) dyes which are always accompanied by aggregation-caused quenching (ACQ) properties, materials with AIE properties are nearly nonluminescent in solution state but emissive in the aggregated state.[30,31] It is reported that ionized AIE-active compounds are nonemissive in aqueous buffer solution, but become highly emissive upon binding to biomolecules such as proteins, through hydrophobic or electrostatic interactions or other noncovalent interactions.[25,32−34] In 2006, Tang and co-workers first used AIE-active tetraphenylethylene (TPE) derivatives for the detection of bovine serum albumin (BSA);[33] later in 2010, the same group found that a nonemissive tetraphenylethene derivative named sodium 1,2-bis[4-(3-sulfonatopropoxyl)phenyl]-1,2-diphe-nylethene (BSPOTPE) could be induced to emit by human serum albumin (HSA), and thus could be used as a probe for HSA detection.[25] In our previous report, we developed 9,10-bis[4-(3-sulfonatopropoxyl)-styryl]anthracene sodium salt (BSPSA), with aggregation-induced emission (AIE) charateristics, for protein quantification and visualization.[34]

Here, BSPSA was used to investigate the unfolding process of EPO. Compared to the method reported in the literature that used three small molecular probes to research the conformation change of protein,[35] the present method in our paper shows good information of the protein conformation change by using BSPSA only. In addition, the BSPSA was easy to synthesize, and the sensitivity of the EPO detection could achieve 1 nmol. The results showed a stable intermediate was monitored in its unfolding process induced by guanidine hydrochloride (GndHCl, 99.5%), a common protein denaturant. Besides, computational modeling suggests that the BSPSA luminogens dock in the hydrophobic cavity in the EPO folding structures. In combination with the circular dichroism (CD) and molecular modeling, the process of EPO unfolding was clearly shown.

MATERIALS AND METHODS

General Information. All reagents were of analytical reagent grade. 4-Methoxystryrene, palladium(II) acetate, 9,10-dibromoanthracene, 1,3-propanesultone, and K_3PO_4 were purchased from Alfa Aesar. The dry *N*,*N*-dimethylacetamide (DMAc) and guanidine hydrochloride (GndHCl, 99.5%) were from Sigma-Aldrich. The boron tribromide (99.99%), methanol, ethanol, and sodium ethylate were obtained from Sinopharm Chemical Reagent Co. (China). Erythropoietin (EPO) was purchased from Sihuan Biopharmaceutical Co. (China).

The excitation and emission spectra were measured with Perkin-Elmer-LS55 luminescence spectroscopy. The ^{1}H NMR spectra were recorded on a Bruker Avance III 400 MHz spectrometer. Circular dichroism (CD) spectra were recorded on a Jasco J-815 CD spectrometer. The elemental analysis was recorded on VarioEL cube (Elmentar, Germany). MS experiments were carried out with Quattro microtriple quadrupole mass spectrometer (Waters). The UV spectrum was acquired by TU-1901 UV−vis spectrophotometer (Beijing, China). Fluorescence microscope images were recorded on an Olympus IX71 fluorescence microscope (Olympus, Japan).

Synthesis of 9,10-Bis[4-(3-sulfonatopropoxyl)-styryl]-anthracene Sodium Salt (BSPSA). Scheme 1 presents the synthetic route we followed to synthesize BSPSA which was improved according to the literature reports.[34,36] 9,10-Bis(4-hydroxystyryl)anthracene was synthesized on the basis of the literature reports.[34,36] Then, 0.54 g of the 9,10-bis(4-hydroxystyryl)anthracene and 20 mL of ethanol were added into a round-bottom flask under nitrogen. Then, a solution of NaOEt (0.20 g) in ethanol (20 mL) was added to the above mixture with stirring until the solution color turned to orange-red. Subsequently, 1,3-propanesultone (0.37 g) in ethanol (20 mL) was added to the reaction mixture. The reaction mixture was stirred overnight. Then, the yellow product was precipitated out from the solution. After filtration and concentration, the product was washed with ethanol and acetone two times to give 0.78 g (85.4%) of a yellow solid. ^{1}H NMR (400 MHz, DMSO-d_6): δ = 8.37 (m, 4H), 7.96 (d, 2H), 7.74 (d, 4H), 7.53−7.56 (m, 4H), 7.01 (d, 4H), 6.86 (d, 2H), 4.11−4.14 (m, 4H), 2.50−2.58 (m, 4H), 2.01−2.06 (m, 4H).

RESULTS AND DISCUSSION

EPO Quantitation in Solution by BSPSA. BSPSA can be applied to the visual monitoring EPO unfolding process as well as quantitative analysis of EPO. To prove its feasibility, the

dx.doi.org/10.1021/la3048278 | Langmuir 2013, 29, 1956−1962

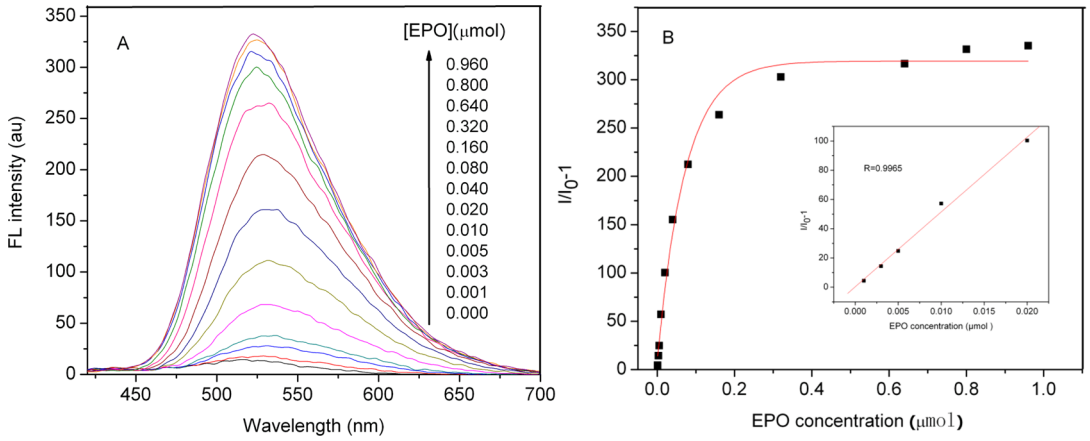

Figure 1. (A) FL spectra of BSPSA containing different amounts of EPO. (B) Change of FL spectra intensity at 522 nm with different amounts of EPO. [BSPSA] = 0.4 μmol; λ_{ex} = 404 nm.

fluorescence (FL) spectra of BSPSA were carried out. Figure 1A shows the FL intensity changes after the addition of different amounts of EPO. It can be seen from Figure 1A that the BSPSA solution is feebly luminescent in the absence of EPO. However, after EPO is added, the BSPSA solution becomes luminescent. The FL spectra intensity keeps rising when the concentration of EPO is increased from 0.001 to 0.8 μM. In addition, the peak shifts from 540 to 522 nm with the increase of EPO; the reason may be attributed to restricted intramolecular motion. BSPSA molecules are aggregated in the hydrophobic cavities of EPO, and then the rotations of the molecules are frozen, which can make the molecular structure of BSPSA much more rigid and BSPSA will become more difficult to be excited. More restricted intramolecular motions can be induced with the increase of EPO, and thus the emission peak of BSPSA shifts toward higher-energy (blue) wavelengths.[37] Figure 1B shows the changes of the rate of the FL spectra intensity with the addition of different amounts of EPO. The rate of the enhancement of FL spectra intensity is faster at low EPO concentrations and then becomes constant when the concentration of EPO is above 0.3 μM. The FL spectra intensity is increased about 350-fold when the concentration of EPO reaches 0.3 μM, and the limit of detection is 1 nM. When the concentration of EPO is increased from 0 to 20 nM, the enhancement in FL spectra intensity is linear to the concentration of EPO with a high correlation coefficient (0.9965). Hence, quantitative analysis of EPO can be fulfilled accordingly. These exciting results show great potential of BSPSA for EPO unfolding process research.

Conformation Studies of EPO by BSPSA. According to reports in the literature we know, a two-state assumption model is usually adopted in kinetic and thermodynamic analysis of EPO unfolding studies.[23,24] In this study, the unfolding process of EPO by guanidine hydrochloride is monitored by utilizing the AIE feature of BSPSA. The results show that three steps are discovered in the unfolding process of EPO. Figure 2 shows the FL intensity changes of BSPSA at 522 nm with increased concentrations of GndHCl in the presence or absence of EPO.

The FL spectra intensity of BSPSA in the absence of EPO is virtually nonluminescent. As control experiments, different amounts of GndHCl are added into BSPSA solution in the absence of EPO; the FL spectra intensity of BSPSA at 522 nm is practically unaffected (○ in Figure 2). However, the FL spectra intensity of BSPSA in the presence of EPO is strongly

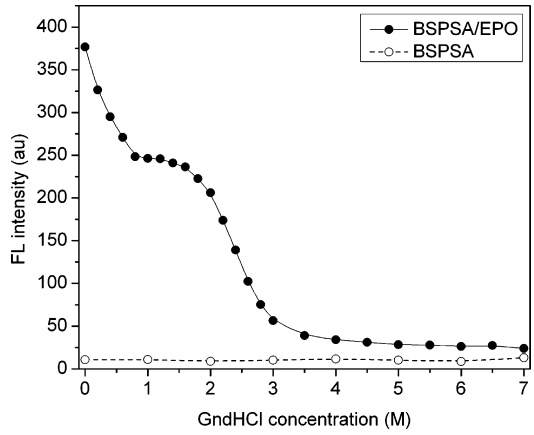

Figure 2. Change of the FL spectra intensity of BSPSA at 522 nm with different concentrations of GndHCl in the presence or absence of EPO. [BSPSA] = 0.4 μmol; [EPO] = 0.85 μmol; λ_{ex} = 404 nm.

luminescent (● in Figure 2). After different amounts of GndHCl are added into BSPSA solution in the presence of EPO, the FL spectra intensity of BSPSA at 522 nm has great changes. In the GndHCl-induced denaturation process, the change is divided into three transition steps. The first transition step appears in the range of GndHCl concentration 0−1.0 M. The FL spectra intensity drops sharply by about 33.3%. The second transition step appears the range of GndHCl concentration 1.0−1.8 M. The FL spectra intensity stays virtually invariant. Then, the FL spectra intensity decreases monotonously along with the addition of GndHCl. When the GndHCl concentration is higher than 4.0 M, the emission is completely quenched. Therefore, a three-state transition for the EPO unfolding process has been discovered. The results demonstrate that the process of EPO unfolding is similar with some other protein unfolding process which was also monitored by utilizing the AIE feature of small molecules.[25]

Conformation Studies of EPO by CD. CD is a common tool for the study of the unfolding process of proteins. Arakawa[23] and Lah[24] studied the thermal-induced EPO unfolding process by the FL technique with CD. Hence, to further confirm the EPO unfolding process, the FL technique with CD is also used for the EPO unfolding study for comparison in this paper. Figure 3A shows the change of CD spectra which shows the secondary structures of EPO after

dx.doi.org/10.1021/la3048278 | Langmuir 2013, 29, 1956−1962

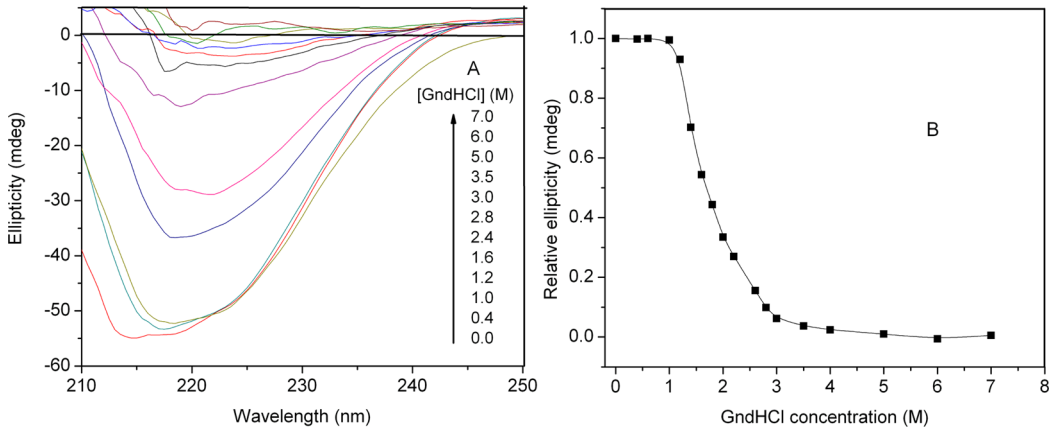

Figure 3. (A) CD spectra of EPO with different amounts of GndHCl. (B) Change of CD spectra intensity at 220 nm with different amounts of GndHCl. [EPO] = 0.85 μmol.

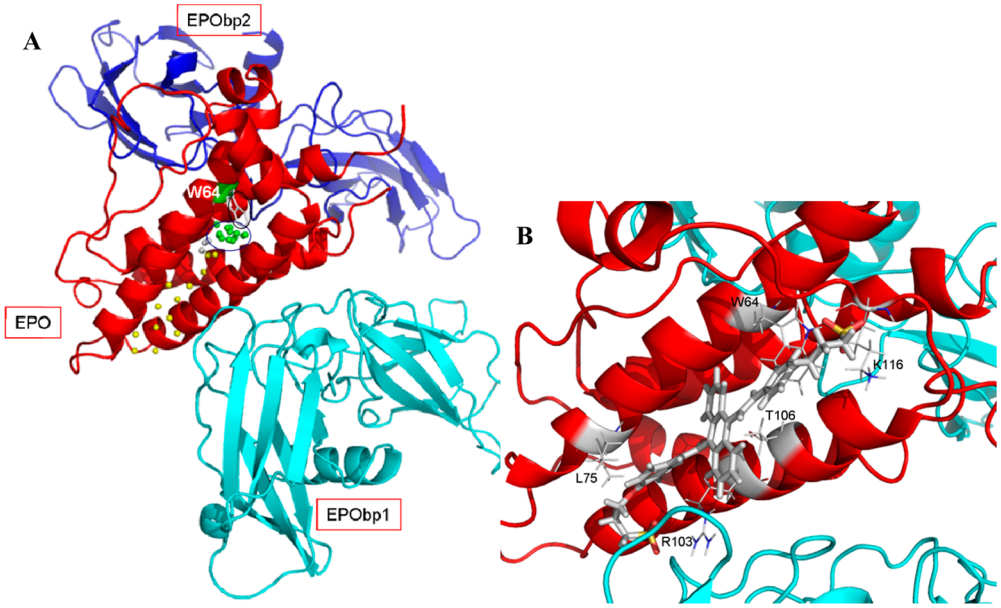

Figure 4. (A) The 45 conformations of BSPSA docked on EPO. The 18 conformations located in the hydrophobic cavity are represented by green ball, and the others are represented by yellow ball. The cavity is shown by blue color cycle. The residue W64 is marked by black color cycle. (B) Details of the binding interactions in one chosen conformation from the 18 conformations. The BSPSA is plotted by a stick representation with a color scheme of gray for carbon, red for oxygen, and yellow for sulfur. The residues interacting with BSPSA are also shown as sticks.

different amounts of GndHCl are added. The CD spectra show the helical contents of EPO. There is no obvious change in the negative ellipticity as the GndHCl concentration is increased from 0 to 1.0 M. Afterward, a much larger change in the secondary structure is observed, which demonstrates that the EPO chains are gradually changed from helical strands to random coils. Figure 3B shows the change of the negative ellipticity of EPO at 220 nm along with the variation of GndHCl concentration. It can be seen from the figure that no intermediate states are monitored by the CD technique. Though CD spectra can provide valuable information about the secondary structures of EPO, details about the tertiary structures cannot be obtained. The plateau of the transition curve in Figure 3B indicates that the secondary structures of EPO remain intact when the concentrations of GndHCl range between 0 and 1.0 M. However, the FL spectral intensity drops sharply in this region (Figure 2) which is inconsistent with the CD spectral data (Figure 3B). This indicates that the tertiary structures are changed in this region of GndHCl concentrations. That the FL spectra intensity staying virtually invariant when the GndHCl concentrations range from 1.0 to 1.8 M hints at the formation of a stable intermediate (Figure 2), which cannot be obtained with the CD spectra data (Figure 3B). Afterward, the EPO strand is unfolded, which is consistent with the CD spectra data. After accomplishment of the EPO unfolding process, the BSPSA molecules are released back to the solution which leads to the obvious decrease of the FL spectra intensity.

Computational Modeling of EPO. Studying the conformation to gain deeper insights into the binding mode and detailed interactions between BSPSA and EPO, the computational modeling is conducted as follows. The structure of BSPSA was evaluated and optimized by free software MOPAC 6, and the crystal structure of EPO was taken from the Protein Data Bank (PDB code 1EER). BSPSA was docked to EPO by AutoDock 4.0 software package[38,39] with an AutoDockTool.[40] For EPO, the Kollman charges, solvation parameters, and polar hydrogen were added. With regard to the ligand BSPSA,

dx.doi.org/10.1021/la3048278 | *Langmuir* 2013, 29, 1956−1962

Gasteiger charges were assigned, and nonpolar hydrogen was merged. Ligand molecules were treated as flexible to enjoy full torsional freedom during modeling. This grid must surround the region of interest in the protein. AutoGrid 4.0 Program, supplied with AutoDock 4.0, was used to generate grid map for the ligand. A default protocol was applied, and the docking between EPO and BSPSA was performed for 45 runs. The resulted 45 docked conformations were summarized and analyzed using AutoDock Tools. Molecular dynamics simulations were performed on the best docked conformation of EPO and BSPSA using GROMACS[41] program to investigate the binding stability of the complex. Following an initial equilibration of 20 ps at 300 K, a 200 ps simulation was carried out at the same temperature. The computational modeling results are showed in Figure 4.

It can be seen from Figure 4A that EPO has an interdomain hydrophobic cavity, and this cavity is adjacent to residue W64. Our docking computations show 18 out of 45 conformations locate in the hydrophobic cavity (circled by blue color liner), and indicate BSPSA has a preference to occur near this structural region. For analysis of the binding interactions between BSPSA and the residues in the cavity, we choose one of these 18 docked conformations and mark the possible residues in Figure 4B. As shown in Figure 4B, the BSPSA reside in the interdomain cleft, and its aromatic rings stack on the above and below helix via some strong hydrophobic interactions. In the binding conformations observed, some residues, such as Arginine(Arg)103, Arg110, and Lysine(Lys)-116 in this cavity, serve as proton donors to form hydrogen bonds with oxygen atoms of the sulfonate group of BSPSA. All the mentioned interactions altogether help to rigidify the molecular conformation of the BSPSA and to prohibit the intramolecular rotation from occurring after being photoexcited, hence making the binding state being highly emissive. The detailed binding modes of the reminding 17 conformations in the hydrophobic cavity closely resemble this one observed. This is expected due to the fact that during docking computations the BSPSA is treated as fully flexible.

Mechanistic Understanding. GndHCl is a common bulky ionic cosolvent for protein research. It can weaken hydrophobic interaction and interfere with association between charged solutes.[42] When EPO unfolds, many nonpolar side chains are exposed to the aqueous medium, but they can be stabilized by GndHCl. After GndHCl enters into the hydrophobic pocket of EPO, the spatial architecture of the protein folds is broken down. The unfolding process of EPO is summarized in Figure 5. During the first unfolding transition, CD spectral data show that the secondary structures of EPO remain intact when the GndHCl concentrations range between 0 and 1.0 M. The sharp dropping of the FL spectra intensity indicates that the tertiary structures are rearranged in this region. Due to the domain being separated, the interdomain hydrophobic pocket is opened. Then, the BSPSA molecules are released into the aqueous medium and become nonemissive because of their unhindered intramolecular rotation. The FL intensity of EPO, therefore, drops sharply.

During the second unfolding transition, the concentrations of GndHCl are in the range 1.0−1.8 M. The FL spectra intensity stays virtually invariant while the CD signal is weakened. In this process, according to the recent reports,[25,43] though parts of the secondary structures have been damaged, the intermediate state may offer additional hydrophobic sites for BSPSA molecules to bind. Because the intradomain contacts may become loose after

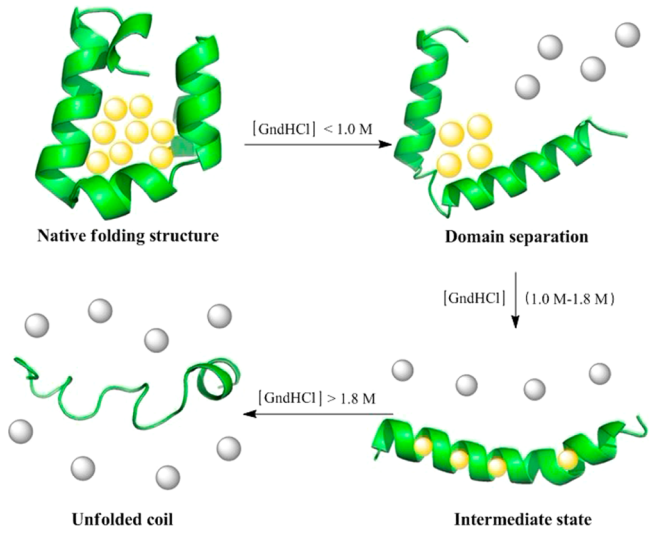

Figure 5. Pictorial model representing the mechanism of EPO unfolding process induced by GndHCl.

domain separation, the BSPSA molecules can enter into the buried hydrophobic patches which are inside the domains more easily. Hence, the curve of FL spectra intensity appears stable in the range 1.0−1.8 M. However, the hydrophobic patches in the EPO protein are completely destroyed because neither secondary structures nor strand helicity is retained when the concentration of GndHCl comes to 4 M. This is confirmed by the CD spectral data. In this process, the solution is feebly luminescent because the BSPSA molecules are completely released from the EPO protein.

■ CONCLUSIONS

In this work, we successfully establish a new convenient method for EPO unfolding research by a synthetically readily accessible and environmentally stable FL molecule named BSPSA. The results indicate that the EPO unfolding process induced by GndHCl is a three-step transition with the intermediate state involved. Compared to the two-state assumption model of EPO unfolding studies, this work exactly describes the EPO unfolding process which is of crucial importance to study the function of EPO. Besides, this work can promote the studies of other biologically important processes by small molecules with AIE characteristics.

■ ASSOCIATED CONTENT

Ⓢ Supporting Information

Additional table, figures, and details. This material is available free of charge via the Internet at http://pubs.acs.org.

■ AUTHOR INFORMATION

Corresponding Author

*E-mail: jinoyang@bnu.edu.cn.

Author Contributions

†These authors contributed equally.

Notes

The authors declare no competing financial interest.

■ ACKNOWLEDGMENTS

The authors gratefully acknowledge the support from the National Nature Science Foundation of China (21175014,

91027034, 20975016), National Grant of Basic Research Program of China (No. 2011CB915504).

REFERENCES

(1) Damberger, F. F.; Christen, B.; Perez, D. R.; Hornemann, S.; Wuethrich, K. Cellular Prion Protein Conformation and Function. *Proc. Natl. Acad. Sci. U.S.A.* **2011**, *108*, 17308−17313.
(2) Pavelcik, F.; Vaclavik, J. Performance of Phased Rotation, Conformation and Translation Function: Accurate Protein Model Building with Tripeptidic and Tetrapeptidic Fragments. *Acta Crystallogr., Sect. D* **2010**, *66*, 1012−1023.
(3) Vasil'ev, S.; Bruce, D. A Protein Dynamics Study of Photosystem II: The Effects of Protein Conformation on Reaction Center Function. *Biophys. J.* **2006**, *90*, 3062−3073.
(4) Ahmed, M. A.; Bamm, V. V.; Harauz, G.; Ladizhansky, V. Solid-State NMR Spectroscopy of Membrane-Associated Myelin Basic Protein—Conformation and Dynamics of an Immunodominant Epitope. *Biophys. J.* **2010**, *99*, 1247−1255.
(5) Curtis-Fisk, J.; Spencer, R. M.; Weliky, D. P. Native Conformation at Specific Residues in Recombinant Inclusion Body Protein in Whole Cells Determined with Solid-State NMR Spectroscopy. *J. Am. Chem. Soc.* **2008**, *130*, 12568−12569.
(6) Cristiani, A.; Costa, G.; Cozza, G.; Meggio, F.; Scapozza, L.; Moro, S. The Role of the N-Terminal Domain in the Regulation of the "Constitutively Active" Conformation of Protein Kinase CK2α: Insight from a Molecular Dynamics Investigation. *ChemMedChem* **2011**, *6*, 1207−1216.
(7) Roberts, G. C. K. Folding and Unfolding for Binding: Large-Scale Protein Dynamics in Protein−Protein Interactions. *Biochem. Soc. Trans.* **2006**, *34*, 971−974.
(8) Aapro, M.; Jelkmann, W.; Constantinescu, S. N.; Leyland-Jones, B. Effects of Erythropoietin Receptors and Erythropoiesis-stimulating Agents on Disease Progression in Cancer. *Br. J. Cancer* **2012**, *106*, 1249−1258.
(9) Patel, N. S.; Kerr-Peterson, H. L.; Brines, M.; Collino, M.; Rogazzo, M.; Fantozzi, R.; Wood, E. G.; Johnson, F. L.; Yaqoob, M. M.; Cerami, A.; Thiemermann, C. Delayed Administration of Pyroglutamate Helix B Surface Peptide (pHBSP), a Novel Non-erythropoietic Analog of Erythropoietin, Attenuates Acute Kidney Injury. *Mol. Med.* **2012**, *18*, 719−727.
(10) Ponce, L. L.; Navarro, J. C.; Ahmed, O.; Robertson, C. S. Erythropoietin Neuroprotection with Traumatic Brain Injury. *Pathophysiology* **2012**, *29*, 1156−1166.
(11) Hirschler-Laszkiewicz, I.; Tong, Q.; Waybill, K.; Conrad, K.; Keefer, K.; Zhang, W.; Chen, S. J.; Cheung, J. Y.; Miller, B. A. The Transient Receptor Potential (TRP) Channel TRPC3 TRP Domain and AMP-Activated Protein Kinase Binding Site Are Required for TRPC3 Activation by Erythropoietin. *J. Biol. Chem.* **2011**, *286*, 30636−30646.
(12) Im, S. J.; Yang, S. I.; Yang, S. H.; Choi, D. H.; Choi, S. Y.; Kim, H. S.; Jang do, S.; Jin, K. S.; Chung, Y. K.; Kim, S. H.; Paik, S. H.; Park, Y. C.; Chung, M. K.; Kim, Y. B.; Han, K. H.; Choi, K. Y.; Sung, Y. C. Natural Form of Noncytolytic Flexible Human Fc as a Long-Acting Carrier of Agonistic Ligand, Erythropoietin. *PLoS One* **2011**, *6*, e24574.
(13) Watson, C.; Sharp, J. S. Conformational Analysis of Therapeutic Proteins by Hydroxyl Radical Protein Footprinting. *AAPS J.* **2012**, *14*, 206−217.
(14) Merstorf, C.; Cressiot, B.; Pastoriza-Gallego, M.; Oukhaled, A.; Betton, J. M.; Auvray, L.; Pelta, J. Wild Type, Mutant Protein Unfolding and Phase Transition Detected by Single-Nanopore Recording. *ACS Chem. Biol.* **2012**, 7,652−7,658.
(15) Bornschlogl, T.; Rief, M. Single-Molecule Protein Unfolding and Refolding Using Atomic Force Microscopy. *Methods Mol. Biol.* **2011**, *783*, 233−250.
(16) Andrade, C. A.; de Oliveira, H. P.; Oliveira, M. D.; Correia, M. T.; Coelho, L. C.; de Melo, C. P. Protein Unfolding Studied by Fluorescence Methods and Electrical Impedance Spectroscopy: The Cases of Cratylia Mollis and Concanavalin A. *Colloids Surf., B* **2011**, *88*, 100−107.
(17) Printz, M.; Friess, W. ltaneous Detection and Analysis of Protein Aggregation and Protein Unfolding by Size Exclusion Chromatography with Post Column Addition of the Fluorescent Dye BisANS. *J. Pharm. Sci.* **2012**, *101*, 826−837.
(18) Rajib, K. M.; Sudarson, S. S.; Samir, K. P. Hydration in Protein Folding: Thermal Unfolding/Refolding of Human Serum Albumin. *Langmuir* **2007**, *23*, 10224−10229.
(19) Pieters, S.; De Beer, T.; Kasper, J. C.; Boulpaep, D.; Waszkiewicz, O.; Goodarzi, M.; Tistaert, C.; Friess, W.; Remon, J. P.; Vervaet, C.; Vander Heyden, Y. Near-Infrared Spectroscopy for In-Line Monitoring of Protein Unfolding and Its Interactions with Lyoprotectants during Freeze-Drying. *Anal. Chem.* **2012**, *84*, 947−955.
(20) Nolting, B.; Andert, K. Mechanism of Protein Folding. *Proteins: Struct., Funct., Bioinf.* **2000**, *41*, 288−298.
(21) Santra, M. K.; Banerjee, A.; Krishnakumar, S. S.; Rahaman, O.; Panda, D. Multiple-Probe Analysis of Folding and Unfolding Pathways of Human Serum Albumin—Evidence for A Framework Mechanism of Folding. *Eur. J. Biochem.* **2004**, *271*, 1789−1797.
(22) Ahmad, B.; Ahmed, M. Z.; Haq, S. K.; Khan, R. H. Guanidine Hydrochloride Denaturation of Human Serum Albumin Originates by Local Unfolding of Some Stable Loops in Domain III. *Biochim. Biophys. Acta* **2005**, *1750*, 93−102.
(23) Arakawa, T.; Philo, J. S.; Kita, Y. Kinetic and Thermodynamic Analysis of Thermal Unfolding of Recombinant Erythropoietin. *Biosci., Biotechnol., Biochem.* **2001**, *65*, 1321−1327.
(24) Lah, J.; Prislan, I.; Krzan, B.; Salobir, M.; Francky, A.; Vesnaver, G. Erythropoietin Unfolding: Thermodynamics and Its Correlation with Structural Features. *Biochemistry* **2005**, *44*, 13883−13892.
(25) Hong, Y. N.; Feng, C.; Yu, Y.; Liu, J. Z.; Lam, J. W. Y.; Luo, K. Q.; Tang, B. Z. Quantitation, Visualization, and Monitoring of Conformational Transitions of Human Serum Albumin by a Tetraphenylethene Derivative with Aggregation-Induced Emission Characteristics. *Anal. Chem.* **2010**, *82*, 7035−7043.
(26) Wang, M.; Zhang, G. X.; Zhang, D. Q.; Zhu, D. B.; Tang, B. Z. Fluorescent Bio/Chemosensors Based on Silole and Tetraphenylethene Luminogens with Aggregation-Induced Emission Feature. *J. Mater. Chem.* **2010**, *20*, 1858−1867.
(27) Shimizu, M.; Hiyama, T. Organic Fluorophores Exhibiting Highly Efficient Photoluminescence in the Solid State. *Chem.—Asian J.* **2010**, *5*, 1561−1531.
(28) Qin, A. J.; Lam, J. W. Y.; Tang, B. Z. Luminogenic Polymers with Aggregation-Induced Emission Characteristics. *Prog. Polym. Sci.* **2012**, *37*, 182−209.
(29) An, B.; Gierschner, J.; Park, S. Y. π-Conjugated Cyanostilbene Derivatives: A Unique Self-Assembly Motif for Molecular Nanostructures with Enhanced Emission and Transport. *Acc. Chem. Res.* **2012**, *45*, 544−554.
(30) Hong, Y. N.; Lam, J. W. Y.; Tang, B. Z. Aggregation-Induced Emission: Phenomenon, Mechanism and Applications. *Chem. Commun.* **2009**, 4332−4353.
(31) Luo, J. D.; Xie, Z. L.; Lam, J. W. Y.; Cheng, L.; Tang, B. Z.; Chen, H. Y.; Qiu, C. F.; Kwok, H. S.; Zhan, X. W.; Liu, Y. Q.; Zhu, D. B. Aggregation-Induced Emission of 1-Methyl-1,2,3,4,5-pentaphenylsilole. *Chem. Commun.* **2001**, *18*, 1740−1741.
(32) Tong, H.; Hong, Y. N.; Dong, Y. Q.; Häussler, M.; Li, Z.; Lam, J. W. Y.; Dong, Y. P.; Sung, H. H.-Y.; Williams, I. D.; Tang, B. Z. Protein Detection and Quantitation by Tetraphenylethene-Based Fluorescent Probes with Aggregation-Induced Emission Characteristics. *J. Phys. Chem. B* **2007**, *111*, 11817−11823.
(33) Tong, H.; Hong, Y. N.; Dong, Y. Q.; Häußler, M.; Lam, J. W. Y.; Li, Z.; Guo, Z. F.; Guo, Z. H.; Tang, B. Z. Fluorescent "Light-Up" Bioprobes Based on Tetraphenylethylene Derivatives with Aggregation-Induced Emission Characteristics. *Chem. Commun.* **2006**, *35*, 3705−3707.
(34) Wang, F. F.; Wen, J. Y.; Huang, L. Y.; Huang, J. J.; Ouyang, J. A Highly Sensitive "Switch-On" Fluorescent Probe for Protein

Quantification and Visualization Based on Aggregation-Induced Emission. *Chem. Commun.* **2012**, *48*, 7395−7397.
(35) Abou-Zied, O. K.; Al-Shihi, O. I. K. Characterization of Subdomain IIA Binding Site of Human Serum Albumin in Its Native, Unfolded, and Refolded States Using Small Molecular Probes. *J. Am. Chem. Soc.* **2008**, *130*, 10793−10801.
(36) Lu, H. G.; Xu, B.; Dong, Y. J.; Chen, F. P.; Li, Y. W.; Li, Z. F.; He, J. T.; Li, H.; Tian, W. J. Novel Fluorescent pH Sensors and a Biological Probe Based on Anthracene Derivatives with Aggregation-Induced Emission Characteristics. *Langmuir* **2010**, *26*, 6838−6844.
(37) Ren, Y.; Lam, J. W. Y.; Dong, Y. Q.; Tang, B. Z; Wong, K. S. Enhanced Emission Efficiency and Excited State Lifetime Due to Restricted Intramolecular Motion in Silole Aggregates. *J. Phys. Chem. B* **2005**, *109*, 1135−1140.
(38) Morris, G. M.; Goodsell, D. S.; Halliday, R. S.; Huey, R.; Hart, W. E.; Belew, R. K.; Olson, A. J. Automated Docking Using a Lamarckian Genetic Algorithm and an Empirical Binding Free Energy Function. *J. Comput. Chem.* **1998**, *19*, 1639−1662.
(39) Huey, R.; Morris, G. M.; Olson, A. J.; Goodsell, D. S. A Semiempirical Free Energy Force Field with Charge-based Desolvation. *J. Comput. Chem.* **2007**, *28*, 1145−1152.
(40) Sanner, M. F. Python: A Programming Language for Software Integration and Development. *J. Mol. Graphics Modell.* **1999**, *17*, 57−61.
(41) Berendsen, H. J. C.; Vanderspoel, D.; Vandrunen, R. Gromacs-A Message-Passing Parallel Molecular-Dynamics Implementation. *Comput. Phys. Commun.* **1995**, *91*, 43−56.
(42) Rossky, P. J. Protein Denaturation by Urea: Slash and Bond. *Proc. Natl. Acad. Sci. U.S.A.* **2008**, *105*, 16825−16826.
(43) Hong, Y. N.; Lam, J. W. Y.; Chen, S. J.; Tang, B. Z. Aggregation-Induced Emission and Biological Application of Tetraphenylethene Luminogens. *Aust. J. Chem.* **2011**, *64*, 1201−1208.